Hydroxychloroquine for treatment of SARS-CoV-2 infection? Improving our confidence in a model-based approach to dose selection

Samuel LM Arnold, Frederick Buckner
University of Washington, Center for Emerging and Reemerging Infectious Disease (CERID), Seattle, WA, USA

Corresponding author

Samuel Arnold; 750 Republican St. Seattle, WA 98109; 206-221-3441; slarnold@uw.edu

Conflict of interest statement

All authors declared no competing interests for this work.

Funding

No funding was received for this work.

Introduction

In less than six months, COVID-19 has spread from a marketplace in Wuhan, China to over 150 countries and territories of the world. Therapeutics are desperately needed to reduce the morbidity and mortality of this pandemic disease. It has been reported that hydroxychloroquine (HCQ) is active against SARS-CoV-2 in vitro, and this finding was quickly supported by an open label non-randomized clinical trial that provided the first published clinical evidence HCQ may be a treatment option.

Background

In less than six months, COVID-19 has spread from a marketplace in Wuhan, China to over 150 countries and territories of the world. The virus, SARS-CoV-2, infects the lower respiratory tract causing fevers, cough, and pneumonitis. As many as 20% of cases are severe (requiring hospitalization) and approximately 1-2% are fatal (1). Therapeutics are desperately needed to reduce the morbidity and mortality of this pandemic disease. While waiting for unregistered products to go through the testing process, the best opportunity for identifying active therapeutics for immediate use is through repurposing existing drugs. Several candidates have been proposed as treatments, and a large amount of attention has been directed towards remdesivir. However, even if remdesivir efficacy is established with randomized controlled trials (RCTs), limitations imposed by intravenous (IV) administration may prevent its widespread utility. Another candidate is the orally administered antimalarial drug chloroquine (CQ), and it has been reported that CQ was successfully used for the treatment of SARS-CoV-2 infection in China (2). The initial report of CQ efficacy in the clinic was followed by a publication describing a CQ analog, hydroxychloroquine (HCQ), as active against SARS-CoV-2 in vitro as well (3). This finding was quickly supported by an open label non-randomized clinical trial of limited size in France that provided the first published clinical evidence HCQ may be a viable treatment option against COVID-19 (4). Based on these early hints of efficacy, the Food and Drug Administration

This article has been accepted for publication and undergone full peer review but has not been through the copyediting, typesetting, pagination and proofreading process, which may lead to differences between this version and the Version of Record. Please cite this article as doi: 10.1111/CTS.12797

(FDA) issued an Emergency Use Authorization (EUA) for emergency use of oral formulations of hydroxychloroquine sulfate for the treatment of 2019 coronavirus disease (COVID-19).

While CQ and HCQ are considered anti-malarial agents, they have alternative uses in rheumatology for the treatment of systemic lupus erythematosus (SLE) and rheumatoid arthritis (5). Between the two, HCQ is the preferred treatment option due to its improved safety profile. CQ and HCQ are weakly basic 4-aminoquinolines that enter the acidic compartments of host cells, and the concentration of these drugs can accumulate in cells through a process known as lysosomal trapping (6, 7). For the treatment of SARS-CoV-2 infection, a reduction in lysosomal pH is believed to adversely impact multiple stages of viral replication (e.g. membrane fusion, spike protein or ACE2 receptor modifications) (8, 9).

From a pharmacokinetic (PK) standpoint, lysosomal trapping can result in the variable sequestration of drug within tissues, and the total drug concentration in tissue may be much higher than plasma (7). As drugs levels reach a steady state, the relationship between tissue and plasma drug concentrations is represented by a partitioning coefficient (Kp). For the treatment of viral pneumonia, there is a specific interest in how drug levels will vary in the lung. Unfortunately, predicting the impact of lysosomal trapping on drug levels in individual tissues over time is very difficult, and it is not clear if the HCQ maximum concentration (C_{max}) and/or area under the curve (AUC) will be associated with efficacy. A lack of confidence in tissue HCQ concentrations impacts our ability to assess toxicity concerns as well. Chronic HCQ use has been associated with QT prolongation (10, 11), and efforts to model HCQ PK should consider both efficacy and known toxicities associated with treatment.

Despite these challenges, a recent publication described the development of a Simcyp physiologically based pharmacokinetic (PBPK) model to support whether HCQ lung levels will be sufficiently high enough to treat SARS-CoV-2 infection (3). The authors briefly described the development of their model, and the model was validated based on previous studies that characterized HCQ plasma and blood PK after a single HCQ IV and/or oral dose. While the provided information is limited, the authors state that their final PBPK model used a HCQ lung Kp value observed in rats, and a perfusion limited lung model for their HCQ lung simulations. The authors used their final Simcyp PBPK model to simulate HCQ lung concentrations with multiple dosing regimens and recommended a dosing regimen that they believed will provide sufficient HCQ lung concentrations without reaching HCQ levels perceived to be unsafe. Partially based on this report, selected hospitalized patients with confirmed COVID-19 and moderate to severe disease or high risk for progression are being treated with HCQ sulfate 400 mg BID x 1 day followed by 200 mg BID x 4 days (University of Washington Medical Center Infectious Disease Physicians, direct communication).

Moving forward, there are several concerns with the PK model that was used to support the recommended HCQ dosing regimen for the treatment of COVID-19. Over the course of treatment, the average simulated plasma HCQ plasma levels (< 100 ng/mL) with the recommended dosing regimen are well below the in vitro HCQ concentration required to reach 50% of the maximum observed SARS-CoV-2 elimination (EC_{50}) in a Vero cell model of viral infection (3). Furthermore, the lowest concentration in vitro that cleared 100% of SARS-CoV-2 was 6,700 ng/mL. However, the relatively low blood levels are not necessarily a problem as previous studies in dogs have observed that HCQ blood exposure does not necessarily correlate with tissue exposure or pharmacodynamic outcomes (12). For treatment of viral pneumonia, the in vivo efficacy is predicted to be driven primarily by high lung HCQ concentrations. However, the relatively high HCQ lung Kp in the PBPK model used to simulate HCQ human lung concentrations was based on HCQ lung Kp values observed in rat PK studies.

Accurate determination of a Kp value requires the drug reaching a distribution equilibrium with the target tissue (> 3 months for HCQ in rats), and there has been a large amount of observed variability in the reported values (13, 14). Furthermore, the relatively high HCQ lung concentrations were based on a perfusion limited lung model. While the rat PK data suggests that a perfusion limited lung model may be suitable for HCQ, it is not clear what data were used to inform the perfusion limited lung model in the author's Simcyp model. An additional concern is that the initial study focused on how the average unbound lung trough HCQ levels compared to an in vitro EC_{50}. For HCQ treatment of COVID-19, we should be using conservative estimates of HCQ lung levels that rely on the lower end of predicted confidence intervals (CIs). Furthermore, instead of relating the lung HCQ levels to current HCQ EC_{50} values, we believe the HCQ lung concentrations should be compared to the HCQ concentration required to clear 100% of SARS-CoV-2 in vitro (6,700 ng/mL). The current HCQ EC_{50} values vary over time, and the time dependent kinetics of HCQ efficacy have not been characterized in detail (3). However, the HCQ concentration required to clear 100% of SARS-CoV-2 in vitro (6,700 ng/mL) was the same at both time points (24 and 48 hours).

For this study, the published HCQ Simcyp PBPK model was used to initially address our concerns. First, we used the HCQ PBPK model to investigate how differences in HCQ lung Kp will impact simulated HCQ concentrations. Next, the Simcyp population simulator was used to determine how conservative estimates of HCQ lung concentrations (5^{th} percentile) compare to the HCQ in vitro efficacy data. Finally, due to known QT prolongation issues, HCQ heart concentrations were simulated to understand how the unbound HCQ heart C_{max} values may vary with different dosing regimens. Overall, our modeling approach was designed to illustrate the current lack of data to support HCQ PK modeling efforts to predict HCQ dosing for treatment of SARS-CoV-2 infection. PBPK modeling was developed and performed with Simcyp® Simulator (see supplemental).

When a range of HCQ lung Kp values were investigated with the Simcyp HCQ model, changes in HCQ lung Kp did not impact simulated plasma or blood HCQ concentrations. However, the panel of Kp values generated large differences in simulated lung HCQ levels relative to HCQ in vitro efficacy. When HCQ sulfate is dosed at 400 mg BID x 1 day followed by 200 mg BID x 4 days, the unbound HCQ lung troughs simulated with a lung Kp of 44 barely reach levels 5-fold higher than the reported HCQ EC_{50} and levels never reach the value required to clear SARS-Cov-2 in vitro (Table 1). If we assume the HCQ lung Kp value is the same in rats and humans (Kp = 220), unbound HCQ lung troughs were predicted to be well above the in vitro EC_{50}, but HCQ troughs did not reach the minimum value required in vitro for virus elimination. In contrast, the HCQ dosing regimen used in the clinical trial in France, 200 mg TID x 10 days, was predicted to generate unbound lung HCQ troughs at levels that clear the virus in vitro for HCQ lung Kp values ≥ 220 (Table 2). However, it should be noted that 5 days of HCQ dosing were required to reach sufficient HCQ lung concentrations with both dosing regimens. A summary of these results is illustrated in Figure 1. Finally, unbound HCQ heart C_{max} values were predicted with each dosing regimen (Table 3). While HCQ dosing of 200 mg BID x 1 day followed by 200 mg BID x 4 days is predicted to generate a higher unbound HCQ heart C_{max} on day 1, HCQ dosing of 200 mg TID x 10 days will have higher HCQ unbound C_{max} values for the remainder of the study. The differences in HCQ heart C_{max} values are relatively small over the first 5 days, but the unbound HCQ heart C_{max} on day 10 predicted with HCQ 200 mg TID x 10 days is more than 3-fold greater than the value predicted with HCQ 200 mg BID x 1 day followed by 200 mg BID x 4 days.

Summary

When simulated tissue drug concentrations are used to support dosing recommendations, the quality of the data used to inform the time dependent drug distribution to tissues should be carefully considered by the researchers. For the HCQ Simcyp model described in this study, changes in lung Kp values did not impact HCQ blood or plasma concentrations, but the adjustments generated dramatic differences in simulated HCQ lung levels. Multiple preclinical in vivo studies support a relatively large HCQ lung Kp but relying entirely on a rat PK study drastically limits the ability of current HCQ PBPK models to translate in vitro efficacy data to the clinic. Given the complex tissue distribution kinetics of HCQ, any attempts to simulate human HCQ lung levels as a basis for HCQ treatment of COVID-19 should be met with caution at this time.

In the future, additional robust mechanistic data should be acquired to improve our understanding of how HCQ levels will vary throughout the body over time. A previous study has provided strong evidence that lysosomal trapping is responsible for the high HCQ in many tissues (7). The authors used a PBPK modeling approach supported by mouse HCQ tissue PK data to illustrate how HCQ lysosome levels vary across multiple tissues. Furthermore, their model predicted human gut and liver HCQ lysosomal concentrations will exceed 10 mM after a single oral 200 mg dose. Lysosomal trapping is a phenomenon that occurs across many cell types including leukocytes. When leukocytes were compared, HCQ uptake was similar in lymphocytes and polymorphonuclear cells but was greatest in purified monocytes (15). Macrophages are not accurately accounted for with our current Simcyp model, and the prediction accuracy may be improved by explicitly accounting for this phenomenon in the model. Furthermore, SARS-CoV-2 is believed to effect cellular entry via attachment of its virion spike protein to the ACE 2 receptor, and this receptor is commonly found on alveolar cells of the lung epithelium (16). Future studies that characterize HCQ concentrations in human epithelial lining fluid (ELF), plasma, alveolar macrophages, and/or bronchial tissue will significantly improve the confidence in HCQ PK modeling and will be crucial for the development of more advanced HCQ multi-compartment lung models. Additional HCQ PK concerns include the known difference in R- and S- HCQ enantiomer rat tissue distribution, the large amount of variability that has been observed in human B/P values, and an incomplete understanding of the role HCQ metabolites may play in efficacy against SARS-CoV-2 (3, 17). Furthermore, the HCQ simulated PK data has been generated with “healthy” populations that do not necessarily reflect the patient populations that need a treatment option for COVID-19. Many of the patients in urgent need of treatment suffer from co-morbidities such as liver and/or kidney disease, and these diseases are likely to impact HCQ disposition. Finally, concern of HCQ toxicity should also drive dose selection. While there are only a few reports of HCQ associated QT prolongation, it is possible that patients in the most need for a COVID-19 treatment may be more susceptible to HCQ toxicity (10, 11). Given these concerns, the current protocol for HCQ treatment of COVID-19 at the University of Washington Medical Center includes monitoring for heart issues by placing the patients on telemetry to track EKG over the course of treatment (University of Washington Medical Center Infectious Disease Physicians, direct communication). Currently there is not an established HCQ concentration (plasma or heart) that is associated with toxicity concerns, so the Simcyp HCQ model can only account for relative differences in HCQ levels without referring to a toxic threshold.

As researchers acknowledge the current lack of HCQ PK information, they should also carefully consider how in vitro experiments are designed to characterize HCQ efficacy against

SARS-CoV-2. The initial studies characterizing HCQ efficacy against SARS-CoV-2 have been conducted with Vero cells which are kidney epithelial cells that were extracted from an African green monkey. Previous work with MERS-CoV suggests phagocytes may serve as viral reservoirs, and future work should explore the use of monocyte-derived macrophages as a host model to characterize therapeutic efficacy against SARS-CoV-2 (18). In addition, if researchers are going to relate HCQ levels to in vitro efficacy data, we suggest using HCQ concentrations required to eliminate SARS-CoV-2 in vitro and not currently available EC_{50} values that vary over time (3).

In conclusion, we are hopeful that HCQ will provide a much-needed treatment option for COVID-19. However, we do not believe that current PK models can be used to inform a HCQ dose selection with a high degree of certainty, based on HCQ's complex PK and an unclear mechanism of action against SARS-CoV-2. In the future, improved HCQ PK models are needed to increase our confidence in predicting HCQ efficacy, assessing potential drug-drug interactions (DDIs), and identifying possible side-effects such as QT prolongation.

Acknowledgements
The authors thank Professor Wesley Van Voorhis for reviewing the manuscript.

References

(1) Guan, W.J. *et al.* Clinical Characteristics of Coronavirus Disease 2019 in China. *N Engl J Med*, (2020) DOI: 10.1056/NEJMoa2002032.

(2) Gao, J., Tian, Z. & Yang, X. Breakthrough: Chloroquine phosphate has shown apparent efficacy in treatment of COVID-19 associated pneumonia in clinical studies. *Biosci Trends* **14**, 72-3 (2020).

(3) Yao, X. *et al.* In Vitro Antiviral Activity and Projection of Optimized Dosing Design of Hydroxychloroquine for the Treatment of Severe Acute Respiratory Syndrome Coronavirus 2 (SARS-CoV-2). *Clin Infect Dis*, (2020). DOI: 10.1093/cid/ciaa237.

(4) Gautret, P. *et al.* Hydroxychloroquine and azithromycin as a treatment of COVID-19: results of an open-label non-randomized clinical trial. Int J Antimicrob Agents. (2020) DOI: 10.1016/j.ijantimicag.2020.105949.

(5) Wallace, D.J., Gudsoorkar, V.S., Weisman, M.H. & Venuturupalli, S.R. New insights into mechanisms of therapeutic effects of antimalarial agents in SLE. *Nat Rev Rheumatol* **8**, 522-33 (2012).

(6) Fox, R.I. Mechanism of action of hydroxychloroquine as an antirheumatic drug. *Semin Arthritis Rheum* **23**, 82-91 (1993).

(7) Collins, K.P., Jackson, K.M. & Gustafson, D.L. Hydroxychloroquine: A Physiologically-Based Pharmacokinetic Model in the Context of Cancer-Related Autophagy Modulation. *J Pharmacol Exp Ther* **365**, 447-59 (2018).

(8) Savarino, A., Boelaert, J.R., Cassone, A., Majori, G. & Cauda, R. Effects of chloroquine on viral infections: an old drug against today's diseases? *Lancet Infect Dis* **3**, 722-7 (2003).

(9) Vincent, M.J. *et al.* Chloroquine is a potent inhibitor of SARS coronavirus infection and spread. *Virol J* **2**, 69 (2005).

(10) Chen, C.Y., Wang, F.L. & Lin, C.C. Chronic hydroxychloroquine use associated with QT prolongation and refractory ventricular arrhythmia. *Clin Toxicol (Phila)* **44**, 173-5 (2006).

(11) O'Laughlin, J.P., Mehta, P.H. & Wong, B.C. Life Threatening Severe QTc Prolongation in Patient with Systemic Lupus Erythematosus due to Hydroxychloroquine. *Case Rep Cardiol* **2016**, 4626279 (2016).

(12) Barnard, R.A., Wittenburg, L.A., Amaravadi, R.K., Gustafson, D.L., Thorburn, A. & Thamm, D.H. Phase I clinical trial and pharmacodynamic evaluation of combination hydroxychloroquine and doxorubicin treatment in pet dogs treated for spontaneously occurring lymphoma. *Autophagy* **10**, 1415-25 (2014).
(13) McChesney, E.W. Animal toxicity and pharmacokinetics of hydroxychloroquine sulfate. *Am J Med* **75**, 11-8 (1983).
(14) McChesney, E.W., Banks, W.F., Jr. & Fabian, R.J. Tissue distribution of chloroquine, hydroxychloroquine, and desethylchloroquine in the rat. *Toxicol Appl Pharmacol* **10**, 501-13 (1967).
(15) French, J.K., Hurst, N.P., O'Donnell, M.L. & Betts, W.H. Uptake of chloroquine and hydroxychloroquine by human blood leucocytes in vitro: relation to cellular concentrations during antirheumatic therapy. *Ann Rheum Dis* **46**, 42-5 (1987).
(16) Hamming, I., Timens, W., Bulthuis, M.L., Lely, A.T., Navis, G. & van Goor, H. Tissue distribution of ACE2 protein, the functional receptor for SARS coronavirus. A first step in understanding SARS pathogenesis. *J Pathol* **203**, 631-7 (2004).
(17) Tett, S.E., Cutler, D.J., Day, R.O. & Brown, K.F. A dose-ranging study of the pharmacokinetics of hydroxy-chloroquine following intravenous administration to healthy volunteers. *Br J Clin Pharmacol* **26**, 303-13 (1988).
(18) Zhou, J. *et al.* Active replication of Middle East respiratory syndrome coronavirus and aberrant induction of inflammatory cytokines and chemokines in human macrophages: implications for pathogenesis. *J Infect Dis* **209**, 1331-42 (2014).

Figure 1: Time course of simulated unbound HCQ lung trough concentrations relative to in vitro efficacy data with varying HCQ lung Kp values. HCQ lung concentrations were simulated with varying HCQ lung Kp values following HCQ dosing of 200 mg BID x 1 day followed by 200 mg BID x 4 days or 200 mg TID x 10 days. The HCQ simulated concentrations were used to calculate the 90% confidence intervals, and the 5th percentile was used to determine the ratio of unbound HCQ lung trough concentrations to the EC_{50} (R_EC_{50}) (A) and minimum concentration required to eliminate SARS-CoV-2 in vitro (R_Max) (B).

Supplemental Information

Supplemental Material

Table 1: Impact of HCQ lung Kp on lung HCQ levels relative to in vitro efficacy data with HCQ dosing of 400 mg BID x 1 day followed by 200 mg BID x 4 days.

Lung Kp	Day 1 (R_EC_{50}, R_Max)	Day 3 (R_EC_{50}, R_Max)	Day 5 (R_EC_{50}, R_Max)	Day 10 (R_EC_{50}, R_Max)
44 (Default)	3.0, 0.1	4.1, 0.1	5.5, 0.2	3.5, 0.1
100	5.0, 0.2	8.8, 0.3	12.1, 0.4	8.2, 0.3
220 (Previous rat studies) (14)	6.2, 0.2	15.4, 0.6	22.8, 0.8	18.7, 0.7
541 (Kp value in previously published PBPK model) (3)	7.0, 0.3	21.2, 0.8	37.6, 1.4	45.4, 1.6

R_EC_{50}: Ratio of HCQ lung trough concentration (unbound)/EC_{50} (241 ng/mL)

R_Max: Ratio of HCQ lung trough concentration (unbound)/minimum concentration required to eliminate SARS-CoV-2 in vitro (6,700 ng/mL)

Table 2: Impact of HCQ lung Kp on lung HCQ levels relative to in vitro efficacy data with HCQ dosing of 200 mg TID x 10 days.

Lung Kp	Day 1 (R_EC_{50}, R_Max)	Day 3 (R_EC_{50}, R_Max)	Day 5 (R_EC_{50}, R_Max)	Day 10 (R_EC_{50}, R_Max)
44 (Default)	2.3, 0.1	5.1, 0.2	7.3, 0.3	11.9, 0.4
100	3.5, 0.1	10.2, 0.4	15.6, 0.6	26.3, 0.9
220 (Previous rat studies) (14)	4.3, 0.2	16.6, 0.6	28.6, 1.0	53.5, 1.9
541 (Kp value in previously published PBPK model) (3)	4.8, 0.2	22.0, 0.8	43.8, 1.6	101.9, 3.7

R_EC_{50}: Ratio of HCQ lung trough concentration (unbound)/EC_{50} (241 ng/mL)

R_Max: Ratio of HCQ lung trough concentration (unbound)/minimum concentration required to eliminate SARS-CoV-2 in vitro (6,700 ng/mL)

Table 3: Simulated unbound HCQ heart C_{max} values with HCQ dosing of 400 mg BID x 1 day followed by 200 mg BID x 4 days or 200 mg TID x 10 days.

HCQ Dosing Regimen	Unbound C_{max} Day 1 (ng/mL)	Unbound C_{max} Day 3 (ng/mL)	Unbound C_{max} Day 5 (ng/mL)	Unbound C_{max} Day 10 (ng/mL)
400 mg BID x 1 day followed by 200 mg BID x 4 days	20,600	24,100	32,050	21,800
200 mg TID x 10 days	14,450	28,400	40,750	68,500

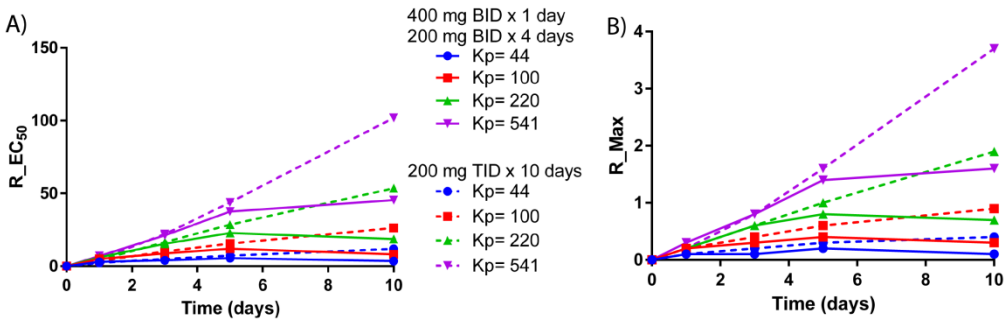

cts_12797_f1.tif